Active Terahertz Modulator and Slow Light Metamaterial Devices with Hybrid Graphene-superconductor Coupled Split-ring Resonator Arrays

S. Kalhor[1], **S. J. Kindness**[2], **R. Wallis**[2], **H. E. Beere**[2], **M. Ghanaatshoar**[3], **R. Degl'Innocenti**[4], **M. J. Kelly**[2, 5], **S. Hofmann**[5] **H. J. Joyce**[5], **D. A. Ritchie**[2], **and K. Delfanazari**[1, 2, 5]

[1]James Watt School of Engineering, University of Glasgow, Glasgow G12 8QQ, UK
[2]Cavendish Laboratory, University of Cambridge, Cambridge CB3 0HE, UK
[3]Laser and Plasma Research Institute, Shahid Beheshti University, Tehran, Iran
[4]Department of Engineering, University of Lancaster, Bailrigg, Lancaster LA1 4YW, UK
[5]Engineering Department, University of Cambridge, Cambridge CB3 0FA, UK

Abstract— The dynamically tunable terahertz (THz) waves and electromagnetically induced transparency (EIT) in coupled hybrid superconducting niobium-graphene split-ring resonator arrays are investigated. Active modulation of THz waves is studied through two different approaches. Thermal tuning of THz amplitude and group delay is observed due to the temperature sensitivity of the niobium superconductor. Stronger photoresponses are observed when niobium is superconducting. The electrical tuning of the integrated hybrid device is accomplished through the integration of graphene patches with the superconducting circuit. The modulation of resonance strength and group delay is observed due to damping of the dark mode resonance in coupled split-ring resonator arrays. The proposed chip-scale device provides a route toward the implementation of active cryogenic THz devices.

1. INTRODUCTION

The demand for efficient and well-designed devices in the range of terahertz (THz) frequencies is originated from the extensive and necessary applications such as the 6th generation of wireless communication, biomedical imaging, security, and sensing [1, 2]. Engineered metamaterials facilitate a wide range of devices with a specific function from filtering to modulating the THz waves [3–6]. A large variety of exotic phenomena can be observed with metamaterials [7–9]. The electromagnetically induced transparency (EIT) as a quantum phenomenon enables the slowing down of the light velocity [10]. It has been shown that the analog of this phenomenon can be obtained in coupled metamaterials due to the destructive interference of two bright-and dark modes [11–15]. The active control of the EIT phenomenon is of interest for practical applications. Actively manipulating the slow light has been reported through dynamically controlling the material properties in semiconductor or superconductor metamaterials [14, 16] and dynamically controlling the surface conductivity of graphene in hybrid metal-graphene metamaterials [17]. Integration of graphene with superconducting metamaterials offers two approaches for the active tuning of the EIT phenomenon [18]: (i) intrinsic tuning of superconducting characteristics via external stimuli such as temperature, magnetic field, and current [19, 20], (ii) the tuning of graphene conductivity via changing the Fermi-level.

In this paper, we present an integrated metamaterial device based on hybrid graphene-superconducting split resonator arrays. Niobium (Nb) superconductor offers the capability of thermal tuning of THz wave amplitude and EIT. Moreover, the integration of graphene with the Nb superconducting circuit provides additional means of active tuning through changing the Fermi level of graphene with the application of back-gate voltages. Therefore, modulation of the EIT response is explored for different graphene conductivities. The proposed chip- scale device can be fabricated in scale and integrated into a single chip [21–24]. Such devices may find applications in the development of solid-state THz devices such as THz-quantum cascade lasers (QCLs) [3, 25], and superconducting intrinsic Josephson junctions (IJJs) THz emitters [26–39].

2. STRUCTURE DESIGN AND METHODS

The metamaterial is based on an array of coupled split-ring resonators (SRRs) made of a 100 nm thick Nb superconductor with a transition temperature of $T_c = 9.2\,\mathrm{K}$ on the SiO_2/Si substrate.

The structure size (shown in Figure 1) is $A = 52\,\mu m$, $B = 42.4\,\mu m$, $C = 46\,\mu m$, $D = 26.8\,\mu m$, $F = 15.6\,\mu m$, $G = 39.6\,\mu m$, $I = 8\,\mu m$, $J = 4\,\mu m$, $W_R = 8\,\mu m$, $W_b = 4\,\mu m$. The periodicity of the structure is set to be $114.4\,\mu m \times 76\,\mu m$. The electromagnetic wave is incident normal to the metamaterial with a polarization parallel to the gap of the split ring, as shown with the blue arrow in Figure 1. There is a patch of graphene in the gap of the upper split ring, and the back-gate voltage (V_{BG}) is used to tune the conductivity of graphene patches. The conductivity of graphene patches changes according to the Drude model $\sigma(\omega) = \frac{\sigma_{DC}}{1+i\omega\tau}$ where $\tau = 15\,fs$ is the scattering time of graphene, and ω is the angular frequency of incident THz wave [17]. The graphene DC conductivity σ_{DC} changes from 0.4 mS to 1.3 mS by applying the back-gate voltage. The measured DC conductivity of graphene (in Table 1) shows that the required back-gate voltage is +100 V for $\sigma_{DC} \cong 0.4\,mS$ and −100 V for $\sigma_{DC} \cong 1.3\,mS$. The transmission of the metamaterial is normalized to the bare substrate (SiO_2/Si) transmission.

Table 1: The measured DC conductivity σ_{DC} of graphene as a function of back-gate voltage.

V_{BG} (V)	−120	−100	−80	−60	−40	−20	0	20	40	60	80	100	120
σ_{DC} (mS)	1.4	1.33	1.25	1.18	1.1	1	0.9	0.78	0.65	0.52	0.44	0.41	0.43

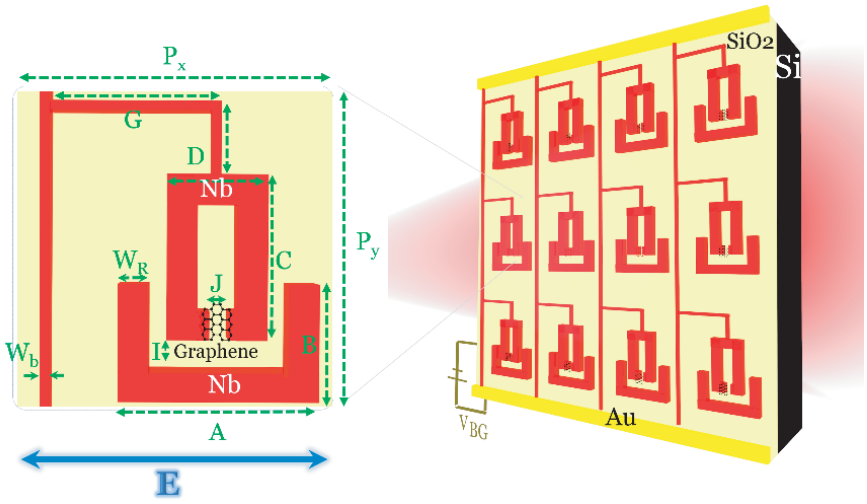

Figure 1: Arrays of coupled graphene-Nb SRRs. Here, Nb, Au, SiO_2, Si, and graphene are shown in red, yellow, gold, black, and gray, respectively. The structure parameters and the polarization of the incident THz wave (blue line) are shown in the Meta-atom figure.

3. RESULTS AND DISCUSSIONS

In the first section, the metamaterial response is investigated in the absence of graphene patches (static superconducting circuit). The THz transmission of the metamaterial for two temperatures of $T = 4.5\,K$ (far from the T_c of Nb) and $T = 10\,K$ (above the T_c of Nb) is shown in Figure 2(a). The first resonance at $f = 0.31\,THz$ is the result of the bias line resonance. In comparison, the second resonance and third resonance are the inductive-capacitive (LC) resonance of lower SRRs and upper SRRs, respectively. The resonance of lower SRRs is called the super-radiant (bright) resonance. On the other hand, the resonance of the upper SRRs is called the sub-radiant (dark) resonance. The transparency window between the dark and bright resonances is obtained as a result of the coupling (destructive interference) of dark and bright resonances.

The characteristic of Nb is primarily affected by the temperature. Nb is in the normal state (lossy metallic state) above its T_c. With decreasing the temperature to below T_c, Nb enters the superconducting state with a large reduction in electronic losses. Therefore, sharper resonance with a larger quality factor and lower transmission minimum is observed for dark and bright resonances when Nb is in the superconducting phase ($T = 4.5\,K$). Moreover, the amplitude of transmission

peak in the EIT window at $f = 0.54\,\mathrm{THz}$ shows an increase with reducing the temperature. The slowing down the group velocity of incident THz waves occurs in the transparency window.

The group delay of the incident wave through the metamaterial is obtained form $t_g = \frac{d\psi}{d\omega}$, where ψ is the phase shift in transmission. The group delay (that is normalized to the group delay of the substrate) for two temperatures is shown in Figure 2(b). The positive group delay shows the decrease in the speed of light in the structure. The reduction in the group delay is observed with increasing the temperature. It is a result of growing losses in the Nb superconductor.

In the second part, the metamaterial response is characterized by the variation of graphene DC conductivities for the temperature of $T = 4.5\,\mathrm{K}$ when Nb is in the superconducting phase. The THz transmission of the metamaterial for different graphene DC conductivities σ_{DC} of 0.4 mS and 1.3 mS is shown in Figure 3(a). The amplitude of dark and bright resonances decreases with adding the graphene patches. The bias line resonance remains unaffected by the variation of graphene DC conductivities. Increasing graphene DC conductivity to $\sigma_{DC} = 1.3\,\mathrm{mS}$ results in decreasing the amplitude of bright and dark resonances. Slowing down the velocity of light in different graphene DC conductivities is shown in Figure 3(b). It shows a reduction in group delay with the integration of graphene patches with the Nb SRRs. With further increasing the graphene DC conductivity to $\sigma_{DC} = 1.3\,\mathrm{mS}$, the group delay reduces.

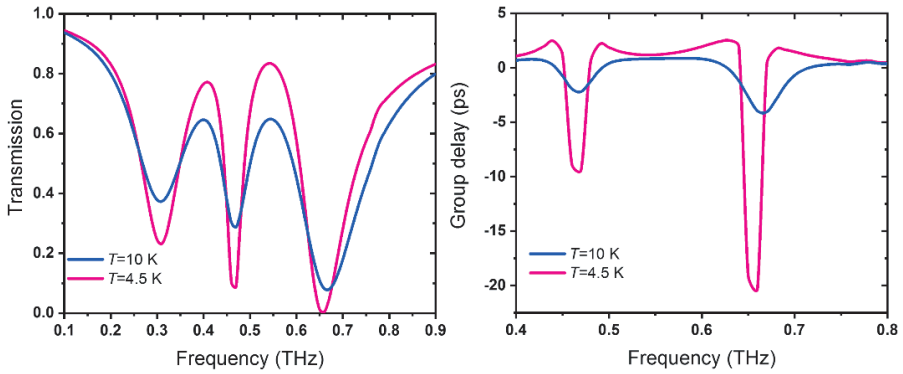

(a) (b)

Figure 2: Thermal evaluation of (a) THz transmission of the metamaterial and (b) the group delay at $T = 4.5\,\mathrm{K}$ (far from the Nb superconducting transition temperature T_c), at $T = 10\,\mathrm{K}$ (where Nb is no longer in the superconducting quantum phase) when there is no graphene in the middle of upper SRRs.

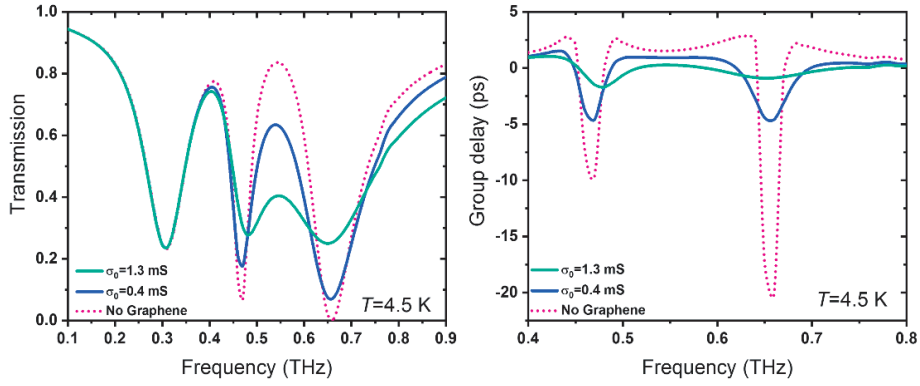

(a) (b)

Figure 3: Electrical evaluation of (a) THz transmission of the metamaterial and (b) the group delay for different graphene DC conductivities of $\sigma_{DC} = 0\,\mathrm{mS}$ (no graphene), 0.4 mS, and 1.3 mS at $T = 4.5\,\mathrm{K}$, far from the Nb superconducting transition temperature.

4. CONCLUSION

We proposed a THz metamaterial based on hybrid graphene-superconductor SRRs arrays. The THz photoresponses of the device were modulated thermally (below the T_c of Nb) and electrically (by tuning the conductivity of graphene). We showed that the THz photoresponses of our proposed hybrid metamaterial device improve when Nb is in the superconducting phase. This device provides a new idea toward the electrically and thermally tunable cryogenic THz devices.

REFERENCES

1. Akyildiz, I. F., J. M. Jornet, and C. Han, "Terahertz band: Next frontier for wireless communications," *Phys. Commun.*, Vol. 12, 16–32, 2014.
2. Mittleman, D. M., "Twenty years of terahertz imaging [Invited]," *Opt. Express*, Vol. 26, No. 8, 9417, 2018.
3. Kindness, S. J., et al., "A terahertz chiral metamaterial modulator," *Adv. Opt. Mater.*, Vol. 8, No. 21, 1–8, 2020.
4. Kalhor, S., M. Ghanaatshoar, T. Kashiwagi, K. Kadowaki, M. J. Kelly, and K. Delfanazari, "Thermal tuning of high-Tc superconducting $Bi_2Sr_2CaCu_2O_8$ terahertz metamaterial," *IEEE Photonics J.*, Vol. 9, No. 5, 1–8, 2017.
5. Kalhor, S., M. Ghanaatshoar, and K. Delfanazari, "On-chip superconducting THz metamaterial bandpass filter," *45th Int. Conf. Infrared, Millimeter, Terahertz Waves*, 1–2, 2020.
6. Keller, J., et al., "High Tc superconducting thz metamaterial for ultrastrong coupling in a magnetic field," *ACS Photonics*, Vol. 5, No. 10, 3977–3983, 2018.
7. Duan, S., et al., "Tunable and high quality factor Fano and toroidal dipole resonances in terahertz superconducting metamaterials," *Mater. Res. Express*, Vol. 7, No. 4, 2020.
8. Lu, F., H. Ou, Y. Liao, F. Zhu, and Y. S. Lin, "Actively switchable terahertz metamaterial," *Results Phys.*, Vol. 15, 102756, Sep. 2019.
9. Yin, Z., et al., "Electrically tunable terahertz dual-band metamaterial absorber based on a liquid crystal," *RSC Adv.*, Vol. 8, No. 8, 4197–4203, 2018.
10. Krauss, T. F., "Why do we need slow light?," *Nat. Photonics*, Vol. 2, No. 8, 448–450, 2008.
11. Nakanishi, T., T. Otani, Y. Tamayama, and M. Kitano, "Storage of electromagnetic waves in a metamaterial that mimics electromagnetically induced transparency," *Phys. Rev. B*, Vol. 87, No. 16, 161110, 2013.
12. Kurter, C., et al., "Classical analogue of electromagnetically induced transparency with a metal-superconductor hybrid metamaterial," Vol. 043901, 1–4, Jul. 2011.
13. Li, C., et al., "Electrical dynamic modulation of THz radiation based on superconducting metamaterials," *Appl. Phys. Lett.*, Vol. 111, No. 9, 2017.
14. Li, C., et al., "Electrically tunable electromagnetically induced transparency in superconducting terahertz metamaterials electrically tunable electromagnetically induced transparency in superconducting terahertz metamaterials," *Appl. Phys. Lett.*, Vol. 119, 052602, 2021.
15. Li, Z., et al., "Manipulating the plasmon-induced transparency in terahertz metamaterials," *Opt. Express*, Vol. 19, No. 9, 8912, 2011.
16. Gu, J., et al., "Active control of electromagnetically induced transparency analogue in terahertz metamaterials," *Nat. Commun.*, Vol. 3, 2012.
17. Kindness, S. J., et al., "Active control of electromagnetically induced transparency in a terahertz metamaterial array with graphene for continuous resonance frequency tuning," *Adv. Opt. Mater.*, Vol. 6, No. 21, 1–8, 2018.
18. Kalhor, S., et al., "Active terahertz modulator and slow light metamaterial devices with hybrid graphene-superconductor photonic integrated circuits," *Nanomaterialsials*, Vol. 11, 2999, 2021.
19. Singh, R. and N. Zheludev, "Superconductor photonics," *Nat. Photonics*, Vol. 8, No. 9, 679–680, 2014.
20. Delfanazari, K. and O. L. Muskens, "Light-matter interactions in chip-integrated niobium nano-circuit arrays at optical fibre communication frequencies," arXiv:2106.11961, 2021.
21. Delfanazari, K., R. A. Klemm, H. J. Joyce, D. A. Ritchie, and K. Kadowaki, "Integrated, portable, tunable, and coherent terahertz sources and sensitive detectors based on layered superconductors," *Proc. IEEE*, Vol. 108, No. 721–734, 2020.
22. Pitsun, D., et al., "Cross coupling of a solid-state qubit to an input signal due to multiplexed dispersive readout," *Phys. Rev. Appl.*, Vol. 14, No. 5, 054059, 2020.

23. Delfanazari, K., et al., "Effect of bias electrode position on terahertz radiation from pentagonal mesas of superconducting $Bi_2Sr_2CaCu_2O_{8+\delta}$," *IEEE Trans. Terahertz Sci. Technol.*, Vol. 5, No. 3, 505–511, 2015.
24. Delfanazari, K., et al., "On-chip hybrid superconducting-semiconducting quantum circuit," *IEEE Trans. Appl., Supercond.*, Vol. 28, No. 4, 1100304, 2018, DOI: 10.1109/TASC.2018.2812817.
25. Kindness, S. J., et al., "External amplitude and frequency modulation of a terahertz quantum cascade laser using metamaterial/graphene devices," *Sci. Rep.*, Vol. 7, No. 1, 1–10, 2017.
26. Welp, U., K. Kadowaki, and R. Kleiner, "Superconducting emitters of THz radiation," *Nat. Photonics*, Vol. 7, No. 9, 702–710, 2013.
27. Tsujimoto, M., et al., "Broadly tunable subterahertz emission from internal branches of the current-voltage characteristics of superconducting $Bi_2Sr_2CaCu_2O_{8+\delta}$ single crystals," *Phys. Rev. Lett.*, Vol. 108, No. 10, 107006, 2012.
28. Xiong, K., Y. Kashiwagi, T. Klemm, R. A. Kadowaki, and K. Delfanazari, "Engineering the cavity modes and polarization in integrated superconducting coherent terahertz emitters," *5th Int. Conf. Infrared, Millimeter, Terahertz Waves*, 1–2, 2020.
29. Delfanazari, K., et al., "Experimental and theoretical studies of mesas of several geometries for terahertz wave radiation from the intrinsic Josephson junctions in superconducting $Bi_2Sr_2CaCu_2O_{8+\delta}$," *37th Int. Conf. Infrared, Millimeter, Terahertz Waves, IRMMW-THz*, 1–2, Sep. 2012.
30. Kadowaki, K., et al., "Quantum terahertz electronics (QTE) using coherent radiation from high temperature superconducting $Bi_2Sr_2CaCu_2O_{8+\delta}$ intrinsic Josephson junctions," *Phys. C Supercond. Its Appl.*, Vol. 491, 2–6, Aug. 2013.
31. Delfanazari, K., et al., "Terahertz oscillating devices based upon the intrinsic josephson junctions in a high temperature superconductor," *J. Infrared, Millimeter, Terahertz Waves*, Vol. 35, No. 1, 131–146, 2014.
32. Kalhor, S., M. Ghanaatshoar, and K. Delfanazari, "Guiding of terahertz photons in superconducting nano-circuits," *2020 Int. Conf. UK-China Emerg. Technol. UCET 2020*, No. 3, 27–29, 2020.
33. Delfanazari, K., et al., "Tunable terahertz emission from the intrinsic Josephson junctions in acute isosceles triangular $Bi_2Sr_2CaCu_2O_{8+\delta}$ mesas," *Opt. Express*, Vol. 21, No. 2, 2171, 2013.
34. Delfanazari, K., et al., "Study of coherent and continuous terahertz wave emission in equilateral triangular mesas of superconducting $Bi_2Sr_2CaCu_2O_{8+\delta}$ intrinsic Josephson junctions," *Phys. C Supercond. Its Appl.*, Vol. 491, 16–19, 2013.
35. Kadowaki, K., et al., Terahertz wave emission from intrinsic Josephson junctions in $Bi_2Sr_2CaCu_2O_{8+\delta}$," *J. Phys: Conf. Ser.*, Vol. 400, No. 2, 022041, 2012.
36. Kashiwagi, T., et. al., "Excitation mode characteristics in Bi2212 rectangular mesa structures," *J. Phys: Conf. Ser.*, Vol. 400, No. 2, 022050, 2012.
37. Tsujimoto, M., et al., "THz-wave emission from inner IV branches of intrinsic Josephson junctions in $Bi_2Sr_2CaCu_2O_{8+\delta}$," *J. Phys: Conf. Ser.*, Vol. 400, No. 2, 022127, 2012.
38. Tsujimoto, M., et al., "Broadly tunable subterahertz emission from internal branches of the current-voltage characteristics of superconducting $Bi_2Sr_2CaCu_2O_{8+\delta}$ single crystals," *Phys. Rev. Lett.*, Vol. 108, 107006, 2012.
39. Elarabi, A., "Circularly polarized terahertz radiation monolithically generated by cylindrical mesas of intrinsic Josephson junctions," *Appl. Phys. Lett.*, Vol. 113, No. 5, 052601.